Journal of Autoimmunity 157 (2025) 103498

Contents lists available at ScienceDirect

Journal of Autoimmunity

journal homepage: www.elsevier.com/locate/jautimm

Alternate splicing converts human CD137 from costimulatory to immunosuppressive function

Manuel Rojas [a,b], Luke S. Heuer [a], Weici Zhang [a], Nicolle Sweeney [a], Carolina Ramírez-Santana [b], Patrick S.C. Leung [a], Alvin Lam [c], Shraddha Kamat [d], Andrew R. Mendelsohn [d], Manley Huang [d], Bo Yu [d], Paulina Ackerman [d], Qisheng Wei [d], James W. Larrick [d], Yi-Guang Chen [e,f], William M. Ridgway [a,*]

[a] Division of Rheumatology, Allergy and Clinical Immunology, University of California, Davis, Davis, CA, United States
[b] Center for Autoimmune Diseases Research (CREA), School of Medicine and Health Sciences, Universidad del Rosario, Bogota, Colombia
[c] California National Primate Research Center, UC Davis, Department of Medical Microbiology and Immunology, School of Medicine, UC Davis, United States
[d] Panorama Research Institute, United States
[e] The Max McGee Research Center for Juvenile Diabetes, Children's Research Institute of Children's Wisconsin, Milwaukee, WI, United States
[f] Division of Endocrinology, Department of Pediatrics, The Medical College of Wisconsin, 8701 Watertown Plank Road, Milwaukee, WI, 53226, United States

ARTICLE INFO

Keywords:
Soluble CD137
CD137
CD137L
4-1BB
4-1BBL
Tnfsf9
Tnfrsf9
Tregs
Tolerance
Autoimmunity

ABSTRACT

Human membrane-bound CD137 (mCD137) is a well-known costimulatory molecule; however, it is alternatively spliced into two transcripts (sCD137-1, 2) whose function is not yet known. Here, we show that sCD137 isoforms lack the CRD4 region and form unique structures compared to mCD137. Human activated Tregs produce both *CD137* splice isoforms, which are rapidly upregulated after cell activation, and identify an activated Treg phenotype along with *FOXP3*, *CTLA4*, and *sCTLA4*. We engineered recombinant Fc-Hu-sCD137 variants, which are immunosuppressive, inhibiting IFN-γ secretion and proliferation in purified $CD4^+$ and $CD8^+$ T cells in an APC-independent manner. These effects are mediated by the downregulation of S6 and 4EBP1 of the mTOR complex 1 pathway. Human sCD137 variants, in contrast to the membrane-bound form, are immunosuppressive and may be a novel treatment for inflammation and autoimmunity.

1. Introduction

The immune system is balanced between activation-mediated effector mechanisms and immunosuppression to prevent over-activation and tissue damage. Homeostasis is maintained by the induction of immunosuppressive counter-regulation as part of the immune activation program. This is illustrated, for example, by costimulatory molecule activation, eg, the upregulation of CTLA-4 after immune activation by CD28 [1]. CD137, also known as 4-1BB, is a membrane-bound costimulatory receptor predominantly expressed on activated T cells. CD137 is a crucial costimulatory molecule for T cell activation, survival, and proliferation. CD137 signaling is mediated via its ligand, CD137L which is widely expressed on both innate and adaptive immune cells [2].

In mice, CD137 plays a major role in both normal immune activation and aberrant function in autoimmune conditions. In the nonobese diabetic (NOD) mouse model of Type 1 Diabetes (T1D), *Cd137* was mapped within the *Idd9.3* region, which prevented T1D [3–7]. The B6 variant of *Idd9.3* protected from T1D by enhancing the survival of $CD137^+$ T regulatory cells (Tregs), which were more immunosuppressive than $CD137^-$ Tregs [8]. We subsequently demonstrated that *Cd137* was the *Idd9.3* susceptibility gene [5]. Production of mouse soluble CD137 (sCD137), a splice isoform of the *Cd137* gene *(Tnfrsf9)* in which the transmembrane region is spliced out, was increased in mice with the B6 allele of *Idd9.3* and in mice effectively treated with an agonist anti-CD137 antibody, suggesting a possible immunomodulatory role of mouse sCD137 [8–11]. Treatment of acutely diabetic NOD mice with sCD137 ameliorates the disease [12]. Mouse sCD137 delayed the onset

* Corresponding author. Division of Rheumatology, Allergy and Clinical Immunology, University of California Davis, School of Medicine, 451 Health Sciences Dr, Suite 6515, Davis, CA, 95616, United States.
E-mail address: wmridgway@health.ucdavis.edu (W.M. Ridgway).

https://doi.org/10.1016/j.jaut.2025.103498
Received 30 September 2025; Received in revised form 30 October 2025; Accepted 2 November 2025
Available online 7 November 2025

of end-stage disease, maintained insulin-producing islet β-cells, and in some cases, prevented the progression to end-stage T1D. The immunological mechanism of sCD137 was anergy induction in $CD4^+$ T cells (reversed by exogenous IL-2), resulting in reduced antigen-specific T cell proliferation and IL-2/IFN-γ secretion *via* mTOR complex 1 (mTORC1) pathway modulation [12]. Additionally, sCD137 significantly lowered inflammatory cytokine production by $CD8^+$ effector memory T cells, which play a key role in β-cell damage. These results suggested that, contrary to mCD137, sCD137 induced a counter-regulatory immunosuppressive response opposing the initial costimulatory action of mCD137. We observed that human T1D patients had lower levels of serum sCD137 compared to age-matched controls [12]. Similar to our findings in mice, human sCD137 is secreted by Tregs, and commercial Fc-sCD137 fusion protein (Leu_{24}-Gln_{186}) suppresses T cell activity in human cells [12]. These results suggested that sCD137 could be a promising avenue for treating T1D and other T cell-mediated autoimmune diseases (ADs) [2].

In humans, two splice isoforms of *CD137 (TNFRSF9)*, referred to as *sCD137-1* and *sCD137-2* have been reported [13]. There is ongoing controversy regarding which RNA isoforms are produced in humans, as various studies have reported conflicting results, suggesting either the presence of both mRNA isoforms or just one [13,14]. However, direct functional studies of the human CD137 splice isoforms and their immunological effects have not been performed; thus, the functional role of these splice isoforms is completely unexplored.

Herein, we provide definitive evidence for the presence and functional expression levels of human CD137 isoforms in primary human peripheral blood mononuclear cells (PBMCs) and T cells. Additionally, we developed novel clinically relevant fusion proteins (i.e., Human Fc-sCD137 variants) and, for the first time, demonstrate that the Fc-sCD137 variants are functionally immunosuppressive, inhibiting both proliferation and inflammatory cytokine production by human T-cells in an mTORC1-dependent manner. The immunosuppressive actions of the splice variants offer a counter-regulatory response to the co-stimulatory actions of the membrane CD137 form. These studies provide proof of concept for a novel immunotherapeutic strategy to treat T-cell-mediated autoimmune conditions such as T1D.

2. Methods

2.1. Sex as a biological variable

Our study examined male and female subjects, and similar findings are reported for both sexes.

2.2. Production, purification, and AlphaFold2 ultrastructure prediction of human Fc-sCD137 variants

Expi293™ cells were transiently transduced with plasmids encoding recombinant human Fc-sCD137-1 and Fc-sCD137-2 cDNA. The secreted Fc-sCD137 proteins were purified independently from the culture supernatants using protein G column affinity chromatography. After elution from the column, purified protein was dialyzed against 1 × 4 L of 1 × Binding buffer, 1 × 4 L of 1 × Binding buffer/1xPBS, then 2 × 4 L of 1 × PBS, and then concentrated using 50 KDa Amicon® Ultra-15 Centrifugal Filter Units (Cat UFC9050). The amount of purified Fc-sCD137 variants was determined by bicinchoninic acid (BCA) Protein Assay (Thermo Scientific™ Pierce™, Cat 23227). SDS-PAGE and western blotting were used to confirm the molecular weight (MW) and homodimer state of the produced proteins. For Fc-sCD137 variants detection by Western blot, primary detection was done by using mouse anti-human CD137 monoclonal antibody (1:2,000, Clone 4B4-1, Biolegend), and secondary detection by goat anti-mouse IgG-HPR (1:20,000, Clone Poly4053, Biolegend). In addition, variants were detected by using goat anti-human IgG-HPR (1:20,000, Clone A18817, Invitrogen).

The binding of Fc-sCD137 variants was tested on human HEK293 cells expressing CD137L-Myc-DDK on the surface as previously described [12]. Briefly, human CD137L-overexpressing HEK293 cells were incubated with recombinant Fc-CD137 variants for 30 min at 37 °C. After washing cells, attached Fc-sCD137 variants were stained with biotinylated anti-human CD137 antibodies (Clone 4B4-1, Biolegend) followed by streptavidin. The level of the bound Fc-sCD137 variant was analyzed by flow cytometry on Agilent NovoCyte 3000 (Beckman Culter).

To predict the ultrastructure of the Fc-sCD137 variants, we used ColabFold v1.5.5. We employed the AlphaFold2 algorithm integrated with the MMseqs2 search tool. The sequences of Fc-CD137-ECD (from R&D), Fc-sCD137-1, and Fc-sCD137-1 were entered into the ColabFold notebook, which uses MMseqs2 to generate a multiple-sequence alignment (MSA) and allows the prediction of protein dimers. This MSA was then fed into the AlphaFold2 model to generate the predicted 3D structure. The specific parameters used within ColabFold, such as the number of cycles and the MSA depth, were kept at their default settings unless otherwise specified. The resulting structural models were then analyzed, and the highest-confidence model, as indicated by the pLDDT scores, was selected for further evaluation of the protein's ultrastructure. This approach leverages the speed and efficiency of MMseqs2 for generating comprehensive MSAs and the accuracy of AlphaFold2 for predicting protein structures.

2.3. PBMC isolation and activation

Whole peripheral blood was collected in BD Vacutainer EDTA tubes (REF: 367863). Then, the PBMCs from healthy donors were separated by centrifugation through the Lymphocyte Separation Medium (Corning, Cat 25-072-CV). Cells were resuspended in 1.5 mL of cell culture media, composed of DMEM media (Gibco, Cat 11965-092) supplemented with 10 % heat-inactivated FBS (Gibco, Cat 10082-147), 100 U/ml of penicillin/streptomycin (Gibco, Cat 15070-063), and 100 nM of sodium pyruvate (Gibco, 11360-070). PBMCs were cultured in a 12-well plate at 3 × 10^6 cells/mL and stimulated with Phytohemagglutinin (PHA) (Sigma, Cat L1668) at 50 μg/mL for 4 days at 37 °C, 5 % CO^2. Cells for RNA extraction and supernatants for sCD137 (R&D Systems, Cat DY838, the ELISA detects total sCD137 protein – including both isoforms 1 and 2) and sCTLA4 (R&D Systems, Cat DY386-05) testing by ELISA were harvested every 24 h after stimulation.

2.4. Human CD137 isoforms sequencing and AlphaFold2 ultrastructure prediction

RNA extraction from recovered PBMCs was performed following RNeasy Mini Kit (QIAGEN, Cat 74104) protocol for further reverse transcription (Applied Biosystems™, Cat 4368814) and cDNA amplification by polymerase chain reaction (PCR) (QIAGEN, Cat 201223). Primers for *CD137* detection and its isoforms were as follows: F-5′-GACTGTTGCTTTGGGACATTTA-3′, R-5′-TCACATCCTCCTTCTTCTTCTTC TC-3`. Temperature conditions for amplification were as follows: 94 °C for 2 min, 94 °C for 45 s X40, 60 °C for 45 s X40, 72 °C for 1min X40, 72 °C for 5 min, 4 °C hold. PCR products were loaded into a 2 % agarose gel and run for 45 min. PCR products for full-length *CD137* (*fCD137*–isoform including the transmembrane and cytoplasmic domain), *sCD137-1*, and *sCD137-2* were isolated from the agarose gel using the QIAquick Gel Extraction Kit (QIAGEN, Cat 28704). Isolated PCR products were ligated to pGEM®-T Easy Vector (Promega Corporation, A1360), transformed into JM109 High-Efficiency Competent Cells (Promega Corporation, L2005), and plated on LB-ampicillin agar plates. Colonies were incubated overnight at 37 °C. The next day, they were tested to confirm the successful transfection of *CD137* isoforms by PCR and then sequenced by Sanger sequencing. We predicted the protein ultrastructure of the isoforms with AlphaFold2, using the same parameters as for the Fc variants (see above for details).

2.5. T cell isolation and activation

PBMCs were isolated as described above. Resting $CD4^+$ T cells were purified by negative selection using a $CD4^+$ T cell isolation kit (Miltenyi Biotec, Cat 130-096-533) following the manufacturer's instructions. To isolate $CD4^+$ T cell subsets, purified $CD4^+$ T cells were stained with PE-conjugated mouse anti-human CD8 (clone SK1, Biolegend), APC-Cy7-conjugated mouse anti-human CD25 (clone BC96, Biolegend), and APC-conjugated mouse anti-human CD127 (Clone A019D5, Biolegend), and sorted using an Astrios (Beckman Coulter). The subsets were defined as follows: $CD4^+$ Tregs ($CD8^-CD25^{hi}CD127^{low}$ cells), and $CD4^+$ Tconv cells ($CD8^-CD25^{low}CD127^{hi}$). Cells were resuspended in 0.2 mL of T cell culture media (TCM), composed of RPMI-1640 media (Gibco, Cat 11875-093) supplemented with 10 % heat-inactivated FBS (Gibco, Cat 10082-147), 10 mM of HEPES (Gibco, Cat 15630-080), 2 mM of L-glutamine (Gibco, Cat 11875-093), 100 U/ml of penicillin/streptomycin (Gibco, Cat 15070-063), 100 nM of sodium pyruvate (Gibco, Cat 11360-070), non-essential amino acids (Gibco, Cat 11140-50), and 150 μM of β-mercaptoethanol (Sigma, M6250). Then, fifty thousand cells were cultured in the presence or absence of 100U/ml of recombinant human IL-2 (R&D, Cat 202-IL-010/CF), and CD3/CD28 Dynabeads (1:4 bead/cell ratio) (Gibco, Cat 11161D) for 4 days at 37 °C, 5 % CO^2. Cells were collected every 24 h for RNA extraction (QIAGEN, Cat 74104), and flow cytometry analysis on Agilent NovoCyte 3000 (Beckman Coulter). Harvested cells were stained for viability with Ghost Dye Violet 510 (Tonbo Biosciences, Cat 13-0870-T100), BV421-conjugated mouse anti-human CD4 (Clone RPA-T4, Biolegend), biotinylated anti-human CD137 antibodies (Clone 4B4-1, Biolegend) followed by streptavidin-PE, FITC-conjugated mouse anti-human FOXP3 (Clone 206D, Biolegend). In addition, supernatants were collected for sCD137 (R&D Systems, Cat DY838) and sCTLA4 (R&D Systems, Cat DY386-05) analysis by ELISA.

2.6. CD137 isoform and Tregs markers by RT-qPCR

RNA extraction from recovered Tconv and Tregs cells was performed using RNeasy Mini Kit (QIAGEN, Cat 74104) protocol for further reverse transcription (Applied Biosystems™, Cat 4368814). Specific primers for each isoform were: *mCD137*: F-5′-TCTTCCTCACGCTCCGTTTCTC-3′, R-5′-TGGAAATCGGCAGCTACAGCCA-3′; *sCD137-1*: F-5′-CGACCCTGGACAAAGACACT-3′, R-5′-AACAGAGAAACGGAGCGTGA-3′; *sCD137-2*: F-5′-GACCCTGGACAAACATTTATGAG-3′, R-5′-CTTCTTCTGGAAATCGGCAGC-3′. The list of primers for the other Treg markers is shown in Supplementary Table 1. Quantitative PCR (qPCR) was done by using Power SYBR™ Green PCR Master Mix (Applied Biosystems™, Cat 4367659). Target gene expression was normalized to *β-ACTIN* expression, and relative expression analysis was done by 2ˆ-ΔΔCT.

2.7. Cytokine secretion, surface markers, and phosphoflow of mTOR pathway in activated human $CD4^+$ and $CD8^+$ T cells treated with Fc-sCD137 variants

Resting total $CD4^+$ and $CD8^+$ T cells were isolated by negative selection using a $CD4^+$ (Miltenyi Biotec, Cat 130-096-533) or $CD8^+$ (Miltenyi Biotec, Cat 130-096-495) T cell isolation kits following the manufacturer's instructions. Cells were resuspended in 0.2 mL of TCM, and fifty thousand cells were cultured on 96-well flat-bottom cell culture plates with human CD3/CD28 Dynabeads (1:16 bead/cell ratio) (Gibco, Cat 11161D) in the presence or absence of serially diluted concentrations of Fc-sCD137 variants (12.5 μg/mL to 100 μg/mL), Rapamycin 100 nM (Cell Signaling, Cat #9904), Wortmannin 1 μM (Cell Signaling, Cat #9951), or LY294002 20 μM (Cell Signaling, Cat #9901) for 4 days at 37 °C, 5 % CO^2. Supernatants were recovered, and IFN-γ (Biolegend, Cat 430104) and IL-2 (Biolegend, Cat 431804) levels were measured by ELISA. Harvested cells were stained for viability with Ghost Dye Violet 510 (Tonbo Biosciences, Cat 13-0870-T100), and BV421-conjugated mouse anti-human CD4 (Clone RPA-T4, Biolegend), or PE-conjugated mouse anti-human CD8 (Clone SK1, Biolegend), or FITC-conjugated mouse anti-human CD98 (Clone MEM-108, Biolegend), or FITC-conjugated mouse anti-human CD71 (Clone CY1G4, Biolegend). Stained cells were analyzed on Agilent NovoCyte 3000 (Beckman Culter).

In addition, in a different experiment, resting total $CD4^+$ and $CD8^+$ T cells were isolated and treated the same way as above. After 4 days of incubation, harvested cells were treated with the Transcription Factor Phospho Buffer Set (BD Pharmigen, Cat 563239) for intracellular staining of phosphorylated proteins following the manufacturer's protocol. Briefly, cells were stained for viability before fixation with Ghost Dye Violet 510 (Tonbo Biosciences, Cat 13-0870-T100), and stained after fixation with BV421-conjugated mouse anti-human CD4 (Clone RPA-T4, Biolegend), or FITC-conjugated mouse anti-human CD8 (Clone SK1, Biolegend), or APC-Cy7-conjugated mouse anti-human CD8 (Clone RPA-T8, Biolegend), APC-Conjugated anti-human pAKT(S473) (Clone SDRNR, eBioscience), PE-conjugated rabbit anti-human p4EBP1(T37/46) (Clone 236B4, Cell signaling), and Alexa 488-conjugated rabbit anti-human pS6(S235/236) (Clone D57.2.2E, Cell signaling) overnight. The next day, cells were washed and resuspended in FACS buffer and analyzed on Agilent NovoCyte 3000 (Beckman Culter).

2.8. Cell proliferation assay of human Tconv cells with Fc-sCD137 variants

Resting total $CD4^+$ T cells were purified by negative selection using a $CD4^+$ T cell isolation kit (Miltenyi Biotec, Cat 130-096-533) following the manufacturer's instructions. To isolate $CD4^+$ T cell subsets, purified $CD4^+$ T cells were stained with PE-conjugated mouse anti-human CD8 (clone SK1, Biolegend), APC-Cy7-conjugated mouse anti-human CD25 (clone BC96, Biolegend), and APC-conjugated mouse anti-human CD127 (Clone A019D5, Biolegend), and sorted using an Astrios sorter (Beckman Coulter). Tconv cells ($CD8^-CD25^{low}CD127^{hi}$) were labeled with carboxyfluorescein succinimidyl ester (CFSE, Invitrogen) at 0.5 μM final concentration. Fifty thousand CFSE-labeled Tconv cells were cultured on 96-well flat-bottom cell culture plates with CD3/28 dynabeads (1:16 bead/cell ratio) (Gibco, Cat 11161D) in the presence or absence of 50 or 100 μg/ml of Fc-sCD137 variants for 4 days at 37 °C, 5 % CO^2. CFSE dilution of harvested cells was analyzed on Agilent NovoCyte 3000 (Beckman Culter). In addition, after supernatant recovery, IFN-γ (Biolegend, Cat 430104) and IL-2 (Biolegend, Cat 431804) levels were measured by ELISA.

2.9. Data analysis

All data acquired in flow cytometry were analyzed using FlowJo software version 10.9.0 (FlowJo, LLC), or NovoExpress (Agilent, Santa Clara CA). All statistical analyses were performed using GraphPad Prism version 10 for Windows (GraphPad software) or R V4.3.3. PCA of Treg-related gene expression was conducted with the FactoMineR and factoextra packages in R. Significance testing was done using either the unpaired *t*-test for sample comparisons and ANOVA with post-hoc analysis for repeated measures or multiple comparisons. Results in bar graphs are expressed as the mean ± standard error of the mean. P-values <0.05 were considered statistically significant.

3. Results

3.1. Tregs are the main source of human soluble CD137, and the sCD137-1 and sCD137-2 isoforms have unique predicted structures compared to membrane CD137

We and others previously demonstrated that in mice, the cell surface expression of CD137 identified a unique Treg subset [5,8,15]. $CD137^+$ Tregs are more suppressive than $CD137^-$ Tregs, demonstrate enhanced survival *in vivo*, and have a significant protective effect in T1D [8–10]. In

humans, Treg expression of membrane CD137 (mCD137) may serve as a marker for Tregs with high *FOXP3* stability after their expansion *in vitro*. In addition, Nowak A et al. [16] demonstrated that human mCD137^{+} Tregs exhibit higher inhibitory activity than mCD137^{-} Tregs, pointing to the critical role of CD137 in human Treg function. However, the role of human *sCD137* isoforms from Tregs and their correlation with other well-known Treg markers such as *FOXP3* and *CTLA4* is unknown.

First, we demonstrated by flow cytometry that human FOXP3^{+} Tregs highly upregulate mCD137 protein levels in the first 24 h post-stimulation compared to T conventional cells (Tconv) (Fig. 1A). The timing of peak protein expression for total sCD137 (by ELISA) and mCD137 (by flow cytometry) aligned with the mRNA peaks for the sCD137 isoforms (by RT-qPCR), with peak levels occurring at 24 h post-stimulation. (Fig. 1B). The *sCD137-1* and *sCD137-2* splice isoforms were upregulated 24- and 48-h post-stimulation, almost entirely in Tregs (Fig. 1B). To confirm the specificity of the isoform primer sets, RT-PCR products were run on an agarose gel to verify single amplification products at the appropriate sizes. (Fig. 1C). The mRNA levels for *mCD137* were higher than for soluble isoforms, and *sCD137-1* levels exceeded *sCD137-2*, reflecting either preferential expression of the membrane-bound form or potential differences in splicing efficiency or primer amplification.

We showed that unfractionated PHA-stimulated human peripheral blood mononuclear cells (PBMCs) produce sCD137 (Supplementary Fig. 1A); however existing sCD137 ELISAs do not differentiate between isoforms 1 and 2. Using primers that spanned the entire splicing region, we evaluated isoform expression using conventional RT-PCR, which yielded three products after amplification that correspond to sizes predicted for full-length CD137 (*fCD137*: unspliced isoform), *sCD137-1*, and *sCD137-2* (Supplementary Fig. 1B). Amplification was stronger at 48 h post-stimulation, correlating with the protein concentration in the supernatants (Supplementary Fig. 1A). To confirm that these bands were the human splice isoforms, PCR products were isolated, ligated with pGEM®-T Easy Vector, cloned into JM109 high-efficiency competent cells, and sequenced. Nucleotide sequencing revealed a larger product of 407 bp and two smaller products of 276 bp and 141 bp, respectively (Supplementary Fig. 1C). The 276 bp product (sCD137-1) has a 131-base deletion (414–544), which encodes a segment of the cysteine-rich domain 4 (CRD4) region and the total length of the Ser/Thr/Pro(STP)-rich segment. This deletion led to a frameshift mutation, with a downstream stop codon (i.e., TAA) resulting in the absence of the transmembrane domain and a different CRD4 configuration (Fig. 2A). The 141 bp product (sCD137-2) has a 255-base deletion that starts at 414 but extends up to 668, compromising a portion of the CRD4 domain, the STP-rich segment, and the transmembrane domain (Supplementary Fig. 1). Both isoforms have unique predicted post-spliced amino acid sequences (Fig. 2A). We employed AlphaFold2 to predict the structural conformations of the isoforms. For comparison, we modeled the extracellular domain (ECD) of fCD137, encompassing amino acids (AAs) spanning CRD1 to CRD4 (Fig. 2A). Modelling predicted significant variation in the isoform structures compared to the ECD of mCD137, and unique regions of the isoforms exhibit low predicted local Distance Difference Test (pLDDT) scores, suggesting these regions are either highly flexible, intrinsically disordered, or lack a well-defined structure.

3.2. *CD137 isoforms contribute to a unique activated Treg fingerprint*

To examine *CD137* splice isoform expression as a predictor of Treg function, we also measured archetypal Treg genes. As expected, *FOXP3*, *CTLA4*, and *sCTLA4* were upregulated in Tregs compared to Tconv, whereas there was no significant difference in expression of *IL-10*, *NFκB*, *TGFβ*, or *ICOS* (Fig. 2B). CD137 splice isoforms cluster strongly with

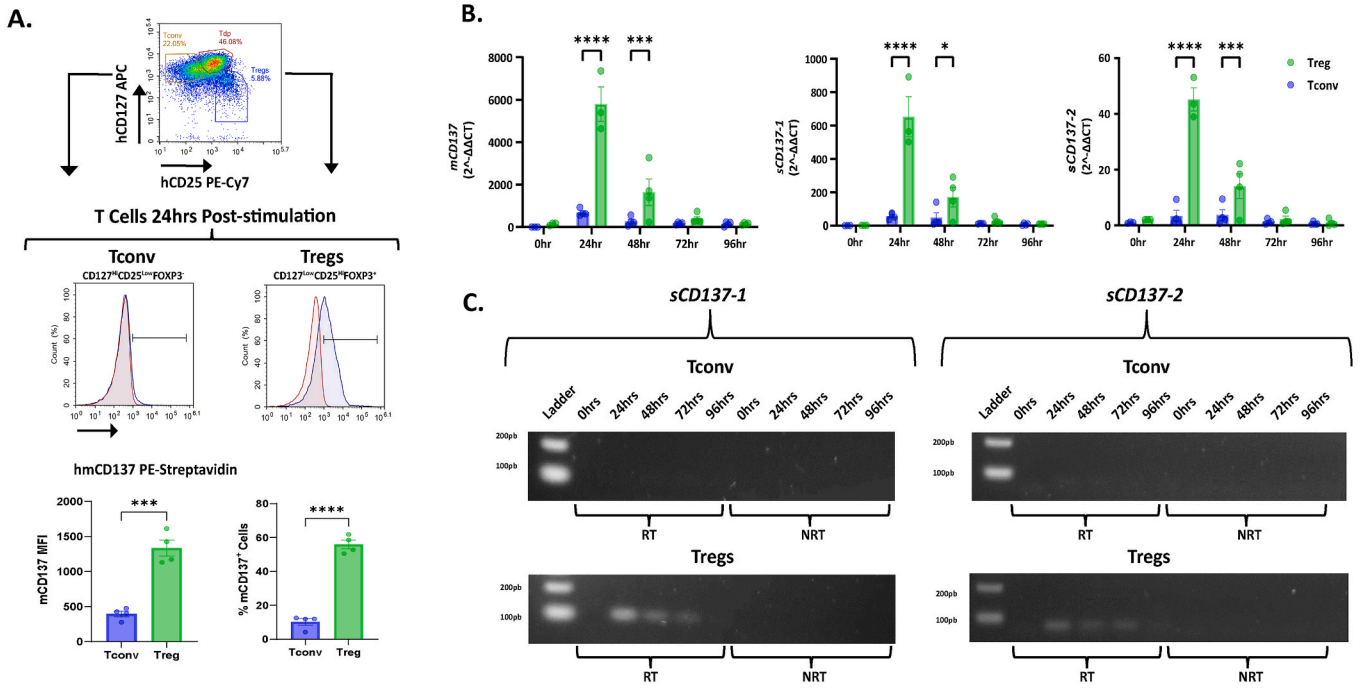

Fig. 1. Tregs highly express sCD137 isoforms. **A**, **B**. FACS and RT-qPCR analysis of T cell CD137 expression. T regulatory (Tregs, CD4^{+} CD25^{Hi}CD127^{Low}), and conventional T cells (Tconv, CD4^{+}CD25^{Low}CD127^{Hi}) were sorted and then cultured in the presence or absence of 100U/ml of IL-2 and CD3/28 dynabeads (1:4 bead/cell ratio) for 4 days (n: 3–4 from four independent experiments). Cells were collected every 24 h for RNA extraction and flow cytometry. Staining of FOXP3 was performed after 24 h mCD137 was evaluated by flow cytometry (**A**) and qPCR (**B**) at baseline, 24 h, and 96 h post-stimulation. Tregs exhibited the highest expression of mCD137, which correlated with qPCR data. Notably, Tregs expressed CD137-1 and CD137-2 isoform transcripts during the first 24 h post-stimulation and returned to baseline after 96 h of stimulation. **C**. Amplification of splice variant cDNA from Tconv and Tregs. The expected sizes for each isoform are sCD137-1 107bp and sCD137-2 79bp. *p < 0.05, **p < 0.005, ***p < 0.0005, ****p < 0.0001 by Two-way ANOVA. Adjusted for multiple comparisons with the Tukey Test. mCD137: Membrane CD137; FMO: Fluorescence minus one; NRT: Non-reverse transcriptase; RT: Reverse transcriptase; RT-qPCR: Real time quantitative PCRsCD137: Soluble CD137.

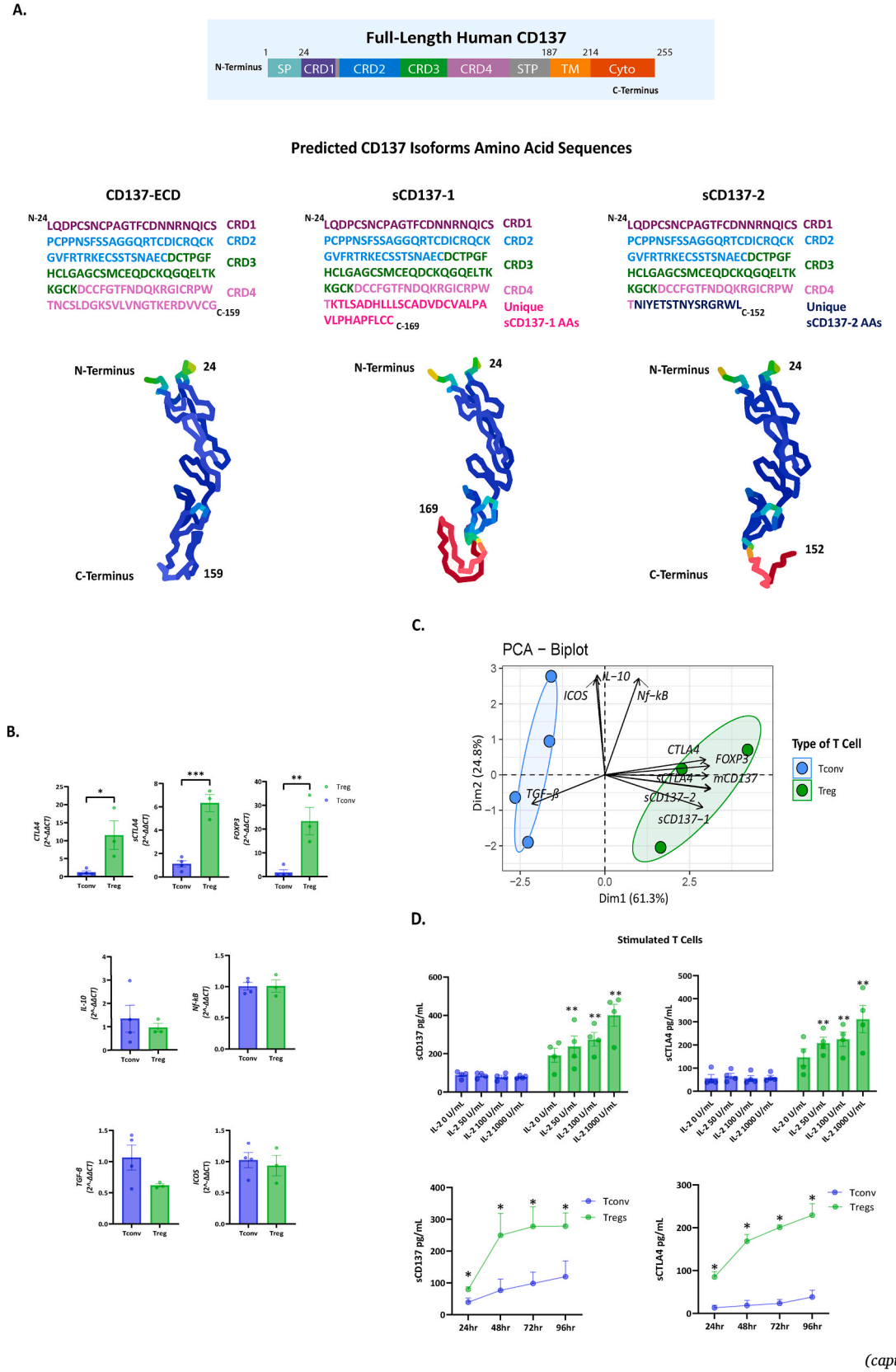

(caption on next page)

Fig. 2. Tregs highly express human sCD137, and the sCD137 isoforms identify an activated Treg phenotype. Predicted sequence of CD137 and its isoforms. The fCD137 is predicted to be 255aa long, sCD137-1 169aa, and sCD137-2 152aa. Splicing variants lack some AAs from the CRD4 and have unique sequences in their C-terminal domain. Colors represent: Blue, pLDDT >90; Light blue, 90 > pLDDT >70; yellow, 70 > pLDDT >50; orange, pLDDT <50. **B.** Expression of other Treg-related genes. *FOXP3*, *CTLA4*, and *sCTLA4* were elevated in Tregs in comparison with Tconv. Transcripts for *IL-10*, *NFKB*, *TGFB*, and *ICOS* did not increase. These transcripts were measured in the same samples at 24hrs post-stimulation as in 2B by RT-qPCR. **C.** Principal component analysis (PCA) of RNA expression of 10 genes at 24 h post-stimulation. *FOXP3*, *mCD137*, *sCD137-1*, *sCD137-2*, *CTLA4*, and *sCTLA4* significantly correlate with a Treg phenotype. **D.** Activated Tregs are the main source of sCD137 and sCTLA4. Tregs and Tconv were sorted and then cultured in the presence or absence of 100U/ml of IL-2 and CD3/28 dynabeads (n: 4 from four independent experiments). Supernatants were collected every 24 h sCD137 reaches a plateau at 48hrs, whereas sCTLA4 increases up to 96hrs. Unstimulated conditions (media only) showed low or negligible levels of sCD137 and sCTLA4 (data not shown but described in text). The sCD137 values represent total protein (isoforms 1 + 2). *p < 0.05, **p < 0.005, ***p < 0.0005 by Two-way ANOVA. Adjusted for mul-tiple comparisons with the Tukey Test. AA: Amino acids; CRD: Cysteine-rich domain; Cyto: Cytoplasmic domain; fCD137: Full-length CD137; CD137-ECD: CD137-Extracellular domain; pLDDT: Predicted local distance difference test; sCD37: Soluble CD137; STP: Ser/Thr/Pro domain; TM: Transmembrane domain; CTLA4: Cytotoxic T-lymphocyte associated protein 4; mCD137: Membrane CD137; FOXP3: Forkhead box P3; ICOS: Inducible T cell co-stimulator; Nf-kB: Nuclear factor kappa-light-chain-enhancer of activated B cells; PCA: Principal component analysis; PCR: Polymerase chain reaction; RT-qPCR: Real time quantitative PCR; sCD137: Soluble CD137; sCTLA4: Soluble CTLA4; TGF-β: Transforming growth factor beta.

these Treg-specific genes (Fig. 2C), forming a unique gene expression phenotype for activated human Tregs. After confirmation of Tregs as the main cell type that expressed transcripts *sCD137* splice isoforms, we confirmed the production of sCD137 in supernatants of activated T cells, as well as the levels of sCTLA4, a well-known regulatory protein produced by Tregs (Fig. 2D). Unstimulated T cells produced low or negligible sCD137 and sCTLA4 (data not shown), while stimulation induced time-dependent increases, with Tregs as the primary source. This confirms that activated Tregs produced higher levels of sCD137 and sCTLA4 than Tconv cells and suggests that they play a pivotal role in the control of inflammation.

3.3. Human Fc-sCD137 variants inhibit the cytokine secretion of activated total CD4$^+$, CD8$^+$, and Tconv cells in vitro

Previous studies confirmed that human T cells express CD137L upon activation, which plays a role in their proliferation and survival [17–19]. To investigate the biological effects of human CD137 isoforms on CD137L in T cells, we developed Fc-sCD137 variants. To avoid unwanted Ig functions, we used a mutant human IgG4 Fc (which does not bind FcγR) that has been engineered to eliminate Fab arm exchange (S228P) and to reduce effector activity (F234A, L235A). Our two novel constructs included 1) Fc-sCD137-1, comprising the AAs 24 to 169 (including the specific AAs for the isoform), and 2) Fc-sCD137-2, comprising the AAs 24 to 152 (including the specific AAs for the isoform). We used AlphaFold2 to predict the structural conformation of the Fc-sCD137 variants. For comparison, we modeled the commercial Fc-CD137-ECD from R&D (i.e., Leu_{24}-Gln_{186}) (R&D, Cat: 838-4B) (Fig. 3A). Modelling predicted significant variation in the Fc variants compared to the predicted Fc-CD137-ECD protein. The Fc-CD137-ECD showed tight alignment of the ECD along the Hu-Fc-IgG1; however, the Fc-sCD137-1 and Fc-sCD137-2 showed divergent structures, forming free arms in opposite directions when forming dimers (Fig. 3A). Thus, the variants manifest specific structural differences, which could affect their biological activity by modifying their interaction with the CD137L.

We confirmed the specificity of the recombinant proteins by Western blot, detecting both human CD137 (using anti-human CD137 antibody, 4B4-1 clone) and human IgG4 (using anti-human IgG-HRP antibody) (Supplementary Fig. 2A). Next, we confirmed the binding of these constructs *in vitro* using HEK-293 human CD137L overexpressing cells (Supplementary Fig. 2B). Variants 1 and 2 showed differential MFIs of binding to the CD137L cells. This could indicate distinct ligand-binding affinities or conformational changes within the protein constructs that influence their recognition by anti-human CD137 antibodies. When using anti-human IgG4 antibodies by flow cytometry, the detection improved, demonstrating that all the variants bound to CD137L (Supplementary Fig. 2B).

We previously demonstrated that mouse recombinant sCD137 induces CD4$^+$ T cell anergy, suppressing antigen-specific T cell proliferation and IL-2/IFN-γ secretion by regulating the mTORC1 pathway in the absence of antigen-presenting cells (APCs) [12]. In this APC-free system, which lacks any APC CD137 or CD137L-mediated co-stimulation of T cells, the suppression by Fc-sCD137 variants indicates an active immunomodulatory effect of soluble CD137 via downregulatory T cell CD137L signaling, rather than passive blockade of co-stimulation. However, there are no studies on the biological activity of human CD137 isoforms and the pathways they regulate. Thus, we evaluated the effects of human Fc-sCD137 variants on activated CD4$^+$ and CD8$^+$ T cells in the absence of APCs.

We stimulated total CD4$^+$ (which includes Tregs) and total CD8$^+$ T cells with CD3/CD28 dynabeads in the presence or absence of Fc-sCD137 variants. The Fc-sCD137 variants significantly reduced IFN-γ secretion of CD4$^+$ and CD8$^+$ cells even at low concentrations; the strongest suppression was in CD8$^+$ T cells (Fig. 3B). However, no effect on IL-2 production was observed in total CD4$^+$ and CD8$^+$ T cells (Data not shown), likely due to the presence of Tregs in the total CD4 population. Therefore, we evaluated the effect of Fc-sCD137 variants on CD4$^+$ Tconv (i.e., CD4$^+$CD25^{low} CD127^{high}) proliferation and cytokine production; using sorted Tconv allowed us to test the suppressive effects of the variants in the absence of Treg cells. Fc-sCD137 variants reduced the proliferation of Tconv cells after activation, as well as the production of both IFN-γ and IL-2 (Fig. 3C). In addition, we tested the additive effect of the two constructs at equal concentrations on activated T cells (i.e., mixing variants 1 and 2). We did not find an additive effect when using this approach (Data not shown). This could be explained by the conserved binding epitope of the sCD137-1 and sCD137-2 to the CD137L (i.e., CRD2-3). Overall, this data confirms that, similar to our mouse experiments, the Fc-sCD137 variants actively suppress T cells via CD137L rather than blocking, given the lack of CD137/CD137L interaction in these assays.

3.4. Human FC-sCD137 variants downregulate the mTORC1 pathway in activated CD4$^+$ and CD8$^+$ cells

Next, we hypothesized that the immunosuppressive effect of Fc-sCD137 variants could act *via* inhibition of the mTOR pathway, as we previously described in mice [12]. First, we evaluated surface receptors regulated by this pathway. CD71 and CD98 are crucial in cell survival and proliferation by regulating intracellular iron and AA transport, respectively [20,21]. The Fc-sCD137 variants reduced the membrane expression of CD71 and CD98 in a concentration-dependent manner in both CD4$^+$ (Fig. 4A) and CD8$^+$ T cells (Fig. 4B).

To further confirm the involvement of the mTOR pathway hypothesis, we quantified the phosphorylation of S6 and 4EBP1 (mTORC1 pathway) and AKT (mTORC2/PI3K) pathways in stimulated CD4$^+$ and CD8$^+$ T Cells. The Fc-sCD137 variants reduced the phosphorylation of S6 and 4EBP1, but not AKT, in both CD4 and CD8 T cells (Fig. 5A and B). Fc-sCD137 variant suppression was comparable to rapamycin (mTORC1 inhibitor) and LY294002 (inhibits both PI3K/Akt and mTOR pathways), but distinct from wortmannin (Specific PI3K/Akt inhibitor), which

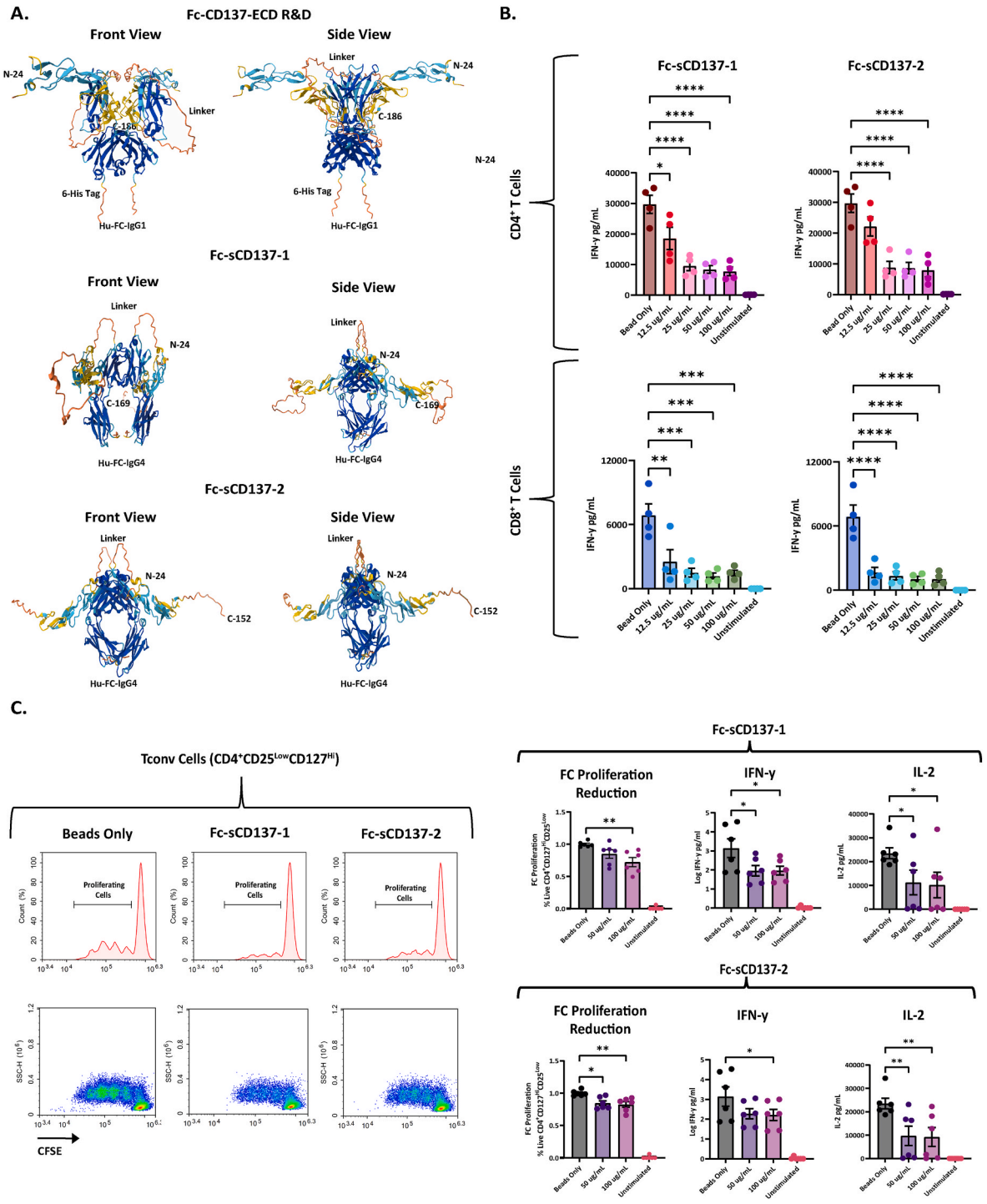

Fig. 3. Fc-sCD137 variants reduce IFN-γ secretion and reduce proliferation of activated CD4^{+}, CD8^{+}, and Tconv cells. A. AlphaFold2 prediction of the ultrastructure of Fc variants. We used the sequence of the commercial Fc-CD137-ECD as a control (R&D, Cat: 838-4B). Modelling predicted significant variation in the Fc variants. The Fc-CD137-ECD showed almost a perfect alignment of the ECD along the Hu-Fc-IgG1; however, the Fc-sCD137-1 and Fc-sCD137-2 showed divergent structures, forming free arms in opposite directions when forming dimers. Colors represent: Blue, pLDDT >90; Light blue, 90 > pLDDT >70; yellow, 70 > pLDDT >50; orange, pLDDT <50. **B.** 50,000 CD4^{+} and CD8^{+} T cells were sorted and then cultured in the presence or absence of CD3/28 dynabeads (1:16 bead/cell ratio) and Fc-sCD137 variants for 4 days (n: 4 from two independent experiments) on a flat-bottom well plate. Cells were collected after 4 days of culture, and viability and cell count were evaluated by flow cytometry. Supernatants were collected and concentrations of IFN-γ and IL-2 were evaluated by ELISA. Fc-CD137 variants reduced the production of IFN-γ but did not modify IL-2 production after four days of culture (Data not shown). **C.** 50,000 FACS-sort purified conventional T cells (Tconv, CD4^{+} CD25^{Hi}CD127^{Low}) were cultured in the presence or absence of CD3/28 dynabeads (1:16 bead/cell ratio) and Fc-sCD137 variants for 4 days on a flat-bottom well plate, and CFSE dilution was evaluated by flow cytometry (n: 6 from two independent experiments). IFN-γ and IL-2 were evaluated in supernatants by ELISA. The concentration of IFN-γ was log-transformed before analysis. FACS plots are one representative. *p < 0.05, **p < 0.005, ***p < 0.0005, ****p < 0.0001 by Two-way ANOVA. Post-hoc comparisons with the Dunnett Test or Fisher's LSD test. CFSE: Carboxyfluorescein succinimidyl ester; ECD: Extracellular domain; FC: Fold change; IFN-γ: Interferon-gamma; IL-2: Interleukin 2; MFI: mean fluorescence intensity; sCD137: Soluble CD137; Tconv: T Conventional.

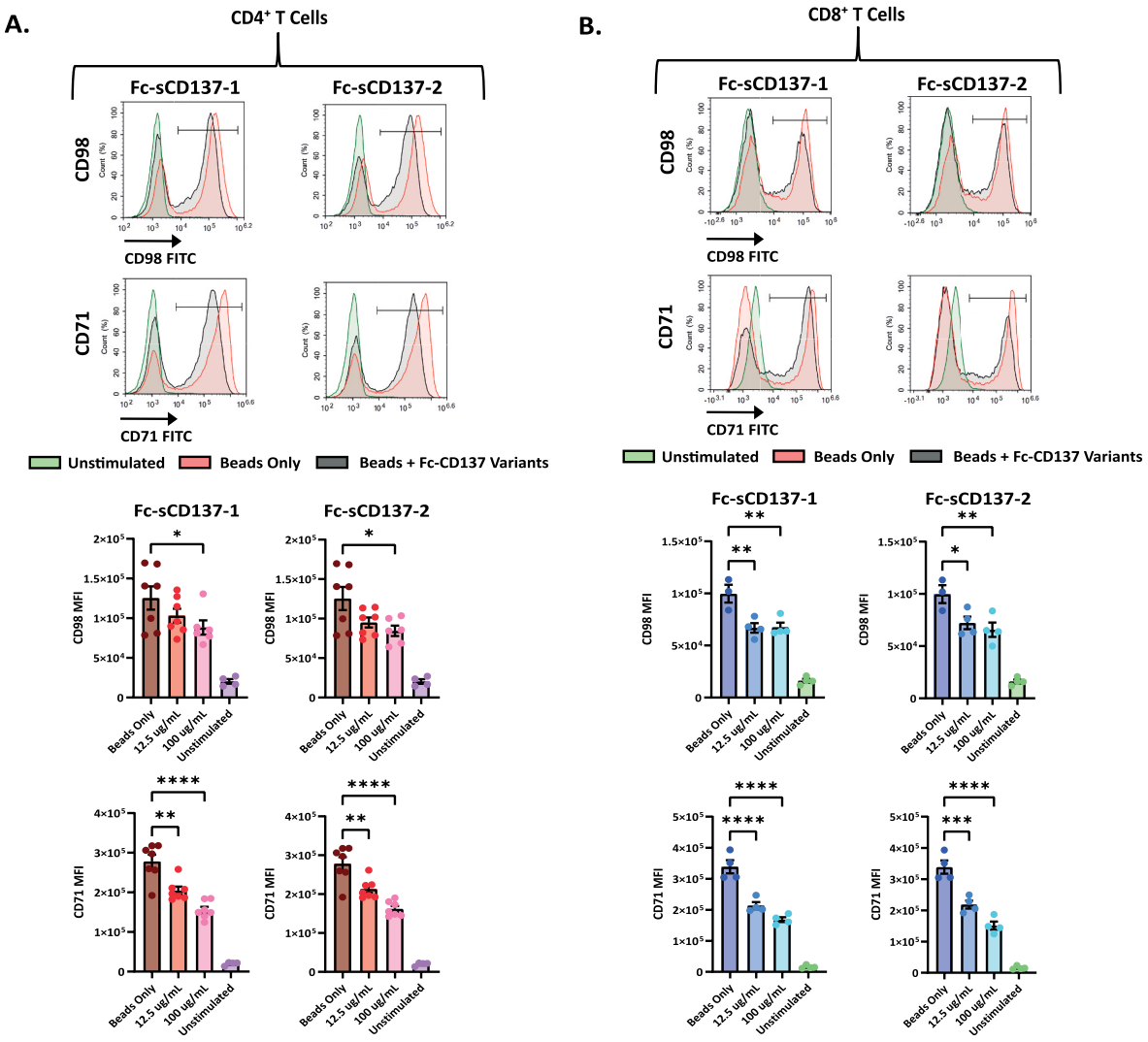

Fig. 4. Fc-sCD137 variants reduce human CD4$^+$ and CD8$^+$ T cells CD98 and CD71 expression. 50,000 CD4$^+$ and CD8$^+$ T cells were sorted and then cultured in the presence or absence of CD3/28 dynabeads (1:16 bead/cell ratio) and Fc-sCD137 variants for 4 days (n: 4 from two independent experiments) on a flat-bottom well plate. Cells were collected after 4 days of culture, and viability and cell count were evaluated by flow cytometry. **A.** MFIs for CD98 and CD71 in CD4$^+$ T cells after 4 days of stimulation. **B.** MFIs for CD98 and CD71 in CD8$^+$ T cells after 4 days of stimulation. FACS plots are representative of 1 single patient (n: 4–7 from two independent experiments). *p < 0.05, **p < 0.005, ***p < 0.0005, ****p < 0.0001 by Two-way ANOVA. Adjusted for multiple comparisons with the Dunnett Test. sCD137: Soluble CD137; MFI: mean fluorescence intensity; sCD137: Soluble CD137.

markedly upregulated pS6 and p4EBP1. This is consistent with our previous results in which mouse sCD137 modulated CD137L signaling in T cells *via* the mTORC1 pathway [12]. The reduction in membrane expression of CD71 and CD98, key transporters involved in iron and AA uptake and crucial for supporting the increased metabolic demands of proliferating T cells [20,21], supports the hypothesis that the soluble Fc-sCD137 variants interfere with cellular metabolism and growth.

4. Discussion

We present here, for the first time, data on the functional activity of novel human CD137 splice variant proteins. Differential splicing events cause unique deletions in the human sCD137 isoforms, resulting in novel protein structures. These novel post-splicing AA sequences differ from murine sCD137 splicing, which only deletes the transmembrane domain, preserving the AA sequence downstream of the deletion [22,23]. The unique AA sequences of these isoforms suggest divergent functional roles of the isoforms.

Human CD137:CD137L interaction requires galectin-9 (Gal-9), which facilitates CD137 aggregation, signaling, and functional activity in T cells, dendritic cells, and natural killer cells [24]. This has significant implications for our understanding of human sCD137 biology since we show here that CD137 (i.e., sCD137-1 and sCD137-2) lack the glycosylation sites in the CRD4 region, which are relevant for the CD137/Gal-9 interaction in mice [25]. Further studies on the functional implication of the CRD4 modifications in the human sCD137 isoforms, their ultrastructure (e.g., homodimer or homotrimer), the modulation of Gal-9, and the sCD137/CD137L interaction are necessary.

Treatment of both CD4$^+$ and CD8$^+$ T cells with the Fc-sCD137 variants significantly reduced IFN-γ secretion, suggesting a potent inhibitory effect of the variants on the Th1-type immune response [26]. In autoimmunity, excessive Th1 responses contribute to tissue damage and inflammation [27], and IFN-γ is critical in differentiating human monocytes into inflammatory M1 macrophages [28]. sCD137 likely regulates the differentiation of inflammatory myeloid cells, either through the reduction of IFN-γ production by T cells or by the direct effect of sCD137 on myeloid CD137L. In mice, a Fc-sCD137 chimera reduced the production of TNF-α after stimulation with LPS [29]. Thus, human sCD137 could affect multiple immune cell subsets. The absence of reduced IL-2 production in the total CD4$^+$ T cell population may be

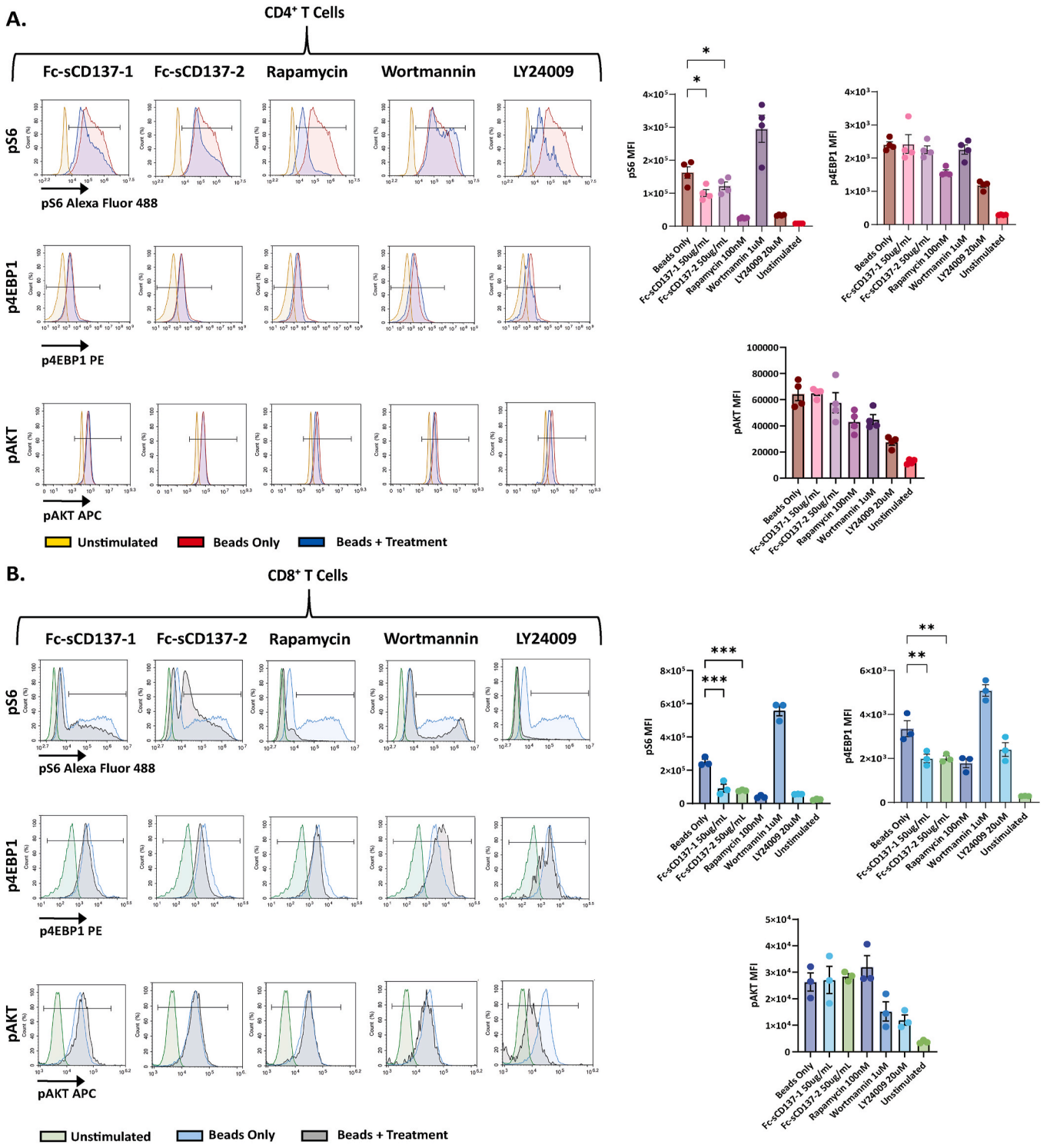

Fig. 5. Fc-sCD137 variants reduce phosphorylation of S6/4 EBP1 in activated human CD4$^+$ and CD8$^+$ T cells. 50,000 CD4$^+$ and CD8$^+$ T cells were sorted and then cultured in the presence or absence of CD3/28 dynabeads (1:16 bead/cell ratio) and Fc-sCD137 variants for 4 days (n: 3–4 from two independent experiments) on a flat-bottom well plate. Cells were collected after 4 days of culture, and geometric MFIs for phosphorylated S6, 4EBP1, and AKT were evaluated by flow cytometry. Horizontal bars represent the gates used for MFI calculation. **A.** Geometric MFIs for phosphorylated S6, 4EBP1, and AKT in CD4$^+$ T Cells. **B.** Geometric MFIs for phosphorylated S6, 4EBP1, and AKT in CD8$^+$ T Cells. FACS plots are representative of one subject (Bar plots show the total n: 3–4 from two independent experiments). *p < 0.05, **p < 0.005, ***p < 0.0005, ****p < 0.0001 by Two-way ANOVA. Adjusted for multiple comparisons with the Holm-Šídák test. sCD137: Soluble CD137; MFI: mean fluorescence intensity.

explained by compensatory IL-2 secretion from other T cell subsets, most likely Tregs [30–32]. Alternatively, the Fc-sCD137 variants may selectively inhibit the IL-2 production of specific effector T cell subsets within the CD4$^+$ population while leaving other subsets unaffected. Further studies are warranted to analyze IL-2 production by specific CD4$^+$ T cell subsets (e.g., Th1, Th2, and Th17 cells) to determine which subsets are most affected by the Fc-sCD137 variants.

The specific inhibition of mTORC1 by these variants offers a

potential advantage over existing immunosuppressive therapies, which often have broader and more pleiotropic effects. Current therapies in autoimmunity targeting mTOR, such as sirolimus (rapamycin) or tacrolimus, bind to the immunophilin FK506 binding protein-12 (FKBP-12) to form an immunosuppressive complex that inhibits mTOR, preventing cell-cycle progression and proliferation [33,34]. However, the inhibition is not cell-specific and may result in side effects such as infections, albeit at a lower rate than broader immunosuppressants like cyclophosphamide, mycophenolate mofetil, and azathioprine [35]. Since sCD137 relies on the expression of CD137L to exert its function [12], the novel Fc-sCD137 variants could offer a more targeted approach to treating inflammation and autoimmunity since they will target only activated T cells. Further *in vivo* and *in vitro* studies are necessary to evaluate whether immunological response against infections is preserved in the presence of Fc-sCD137 variants.

Rapamycin enhances oxidative phosphorylation that modulates the differentiation of FOXP3^{+} Tregs [36] in the presence of strong TCR stimulation [37]. Rapamycin can therefore expand Tregs *in vitro* for therapeutic use [38–40]. In addition, a recent clinical study showed that rapamycin can restore the Treg function in patients with immune-dysregulation, polyendocrinopathy, enteropathy, and X-linked (IPEX) syndrome [41]. As our data showed that Fc-sCD137 variants modulate T cells *via* mTORC1 (similar to rapamycin), they may also preserve and potentiate Tregs to control inflammation. This deserves further study since Fc-sCD137 variants could serve as Treg inducers during expansion for immunotherapy to restore Treg functionality in patients with T1D [42], primary biliary cholangitis [43], or systemic lupus erythematosus [44], enhancing the benefits of this therapy beyond direct immunosuppression of Tconv cells.

We previously demonstrated that recombinant mouse sCD137 inhibits T-cell proliferation [10], and similarly, commercial human Fc-CD137 suppressed the proliferation of activated human Tconv cells [12]. Herein, we confirm that human Fc-CD137 variants suppress proliferation along with the production of inflammatory cytokines in Tconv cells, likely due to suppression of mTORC1. The reduction in membrane expression of CD71 and CD98, key transporters involved in iron and amino acid uptake [20,21], further supports the notion that the Fc-CD137 variants suppress with cellular metabolism and growth. These transporters are crucial for supporting the increased metabolic demands of proliferating T cells [20,21].

While isoforms differ in sequence and predicted structure, they exhibited comparable immunosuppressive functions in our assays, suggesting shared mechanisms via common domains. Future studies are needed to clarify functional or biological differences between the isoforms. Testing the Fc-CD137 variants in humanized models will provide valuable insights into their efficacy and help elucidate their effects in complex immunological interactions. Furthermore, we centered this study on T cells while the effects of Fc-CD137 variants on other immune cell types remain unexplored. For example, the study of their effect on myeloid cells is crucial to a comprehensive understanding of the mechanisms of action for human sCD137 isoforms. Our studies demonstrate the immunosuppressive effects of recombinant sCD137 isoforms. Utilizing supernatants from activated Tregs could further corroborate Tregs as the principal source of sCD137-mediated suppression; however, this approach may be complicated by other suppressive molecules co-expressed by Tregs, as demonstrated in our co-expression analyses (Fig. 2). Furthermore, it would preclude the distinction between the effects of sCD137-1 and sCD137-2 or the accurate quantification of each isoform. Consequently, we focused on recombinant proteins to delineate their specific effects. Prior research has demonstrated the essential function of CD137 in Treg suppressive activity [16]. Subsequent experiments utilizing blocking antibodies against CD137L when using Treg supernatants may yield further insights.

In summary, this study provides novel insights into the human CD137 system, demonstrating the functional immunosuppressive capacities of the human soluble CD137 splice variant proteins (i.e., FC-sCD137-1 and FC-sCD137-2) with functional immunosuppressive effects that counter regulate mCD137 costimulatory effects. We demonstrate that Tregs are the primary source of *CD137* isoforms transcripts and show that recombinant Fc-sCD137 variants exert potent immunosuppressive effects on activated T cells *via* modulation of the mTORC1 pathway. Suppression of mTORC1 via sCD137 may offer significant advantages compared to systemic suppression of mTORC1, eg, by Rapamycin, since sCD137 treatment targets suppression specifically to CD137L-expressing immune cells. These findings significantly advance our understanding of sCD137 in human immune regulation.

CRediT authorship contribution statement

Manuel Rojas: Writing – review & editing, Writing – original draft, Visualization, Validation, Supervision, Software, Resources, Project administration, Methodology, Investigation, Formal analysis, Data curation, Conceptualization. **Luke S. Heuer:** Writing – review & editing, Writing – original draft, Visualization, Validation, Supervision, Software, Resources, Project administration, Methodology, Investigation, Funding acquisition, Formal analysis, Data curation, Conceptualization. **Weici Zhang:** Writing – review & editing, Writing – original draft, Visualization, Validation, Supervision, Software, Resources, Project administration, Methodology, Investigation, Funding acquisition, Formal analysis, Data curation, Conceptualization. **Nicolle Sweeney:** Writing – review & editing, Writing – original draft, Visualization, Validation, Supervision, Software, Resources, Project administration, Methodology, Investigation, Funding acquisition, Formal analysis, Data curation, Conceptualization. **Carolina Ramírez-Santana:** Writing – review & editing, Writing – original draft, Visualization, Validation, Supervision, Software, Resources, Project administration, Methodology, Investigation, Funding acquisition, Formal analysis, Data curation, Conceptualization. **Patrick S.C. Leung:** Writing – review & editing, Writing – original draft, Visualization, Validation, Supervision, Software, Resources, Project administration, Methodology, Investigation, Funding acquisition, Formal analysis, Data curation, Conceptualization. **Alvin Lam:** Writing – review & editing, Writing – original draft, Visualization, Validation, Supervision, Software, Resources, Project administration, Methodology, Investigation, Funding acquisition, Formal analysis, Data curation, Conceptualization. **Shraddha Kamat:** Writing – review & editing, Writing – original draft, Visualization, Validation, Supervision, Software, Resources, Project administration, Methodology, Investigation, Funding acquisition, Formal analysis, Data curation, Conceptualization. **Andrew R. Mendelsohn:** Writing – review & editing, Writing – original draft, Visualization, Validation, Supervision, Software, Resources, Project administration, Methodology, Investigation, Funding acquisition, Formal analysis, Data curation, Conceptualization. **Manley Huang:** Writing – review & editing, Writing – original draft, Visualization, Validation, Supervision, Software, Resources, Project administration, Methodology, Investigation, Funding acquisition, Formal analysis, Data curation, Conceptualization. **Bo Yu:** Writing – review & editing, Writing – original draft, Visualization, Validation, Supervision, Software, Resources, Project administration, Methodology, Investigation, Funding acquisition, Formal analysis, Data curation, Conceptualization. **Paulina Ackerman:** Writing – review & editing, Writing – original draft, Visualization, Validation, Supervision, Software, Resources, Project administration, Methodology, Investigation, Funding acquisition, Formal analysis, Data curation, Conceptualization. **Qisheng Wei:** Writing – review & editing, Writing – original draft, Visualization, Validation, Supervision, Software, Resources, Project administration, Methodology, Investigation, Funding acquisition, Formal analysis, Data curation, Conceptualization. **James W. Larrick:** Writing – review & editing, Writing – original draft, Visualization, Validation, Supervision, Software, Resources, Project administration, Methodology, Investigation, Funding acquisition, Formal analysis, Data curation, Conceptualization. **Yi-Guang Chen:** Writing – review & editing, Writing – original draft, Visualization, Validation, Supervision,

Software, Resources, Project administration, Methodology, Investigation, Funding acquisition, Formal analysis, Data curation, Conceptualization. **William M. Ridgway:** Writing – review & editing, Writing – original draft, Visualization, Validation, Supervision, Software, Resources, Project administration, Methodology, Investigation, Funding acquisition, Formal analysis, Data curation, Conceptualization.

Inclusion and ethics statement

The study was reviewed and approved by the institutional IRB.

Funding information

National Institutes of Health, Grant/Award Number: 1R01DK107541-01A1; National Institute of Diabetes and Digestive and Kidney Diseases.

This work was supported by NIH 1R01DK107541-01A1.

Appendix A. Supplementary data

Supplementary data to this article can be found online at https://doi.org/10.1016/j.jaut.2025.103498.

Data availability

Data will be made available on request.

References

[1] G. Magistrelli, P. Jeannin, N. Herbault, A. Benoit De Coignac, J.F. Gauchat, J. Y. Bonnefoy, Y. Delneste, A soluble form of CTLA-4 generated by alternative splicing is expressed by nonstimulated human T cells, Eur. J. Immunol. 29 (1999) 3596–3602, https://doi.org/10.1002/(SICI)1521-4141(199911)29:11<3596::AID-IMMU3596>3.0.CO;2-Y.

[2] M. Rojas, L.S. Heuer, W. Zhang, Y.-G. Chen, W.M. Ridgway, The long and winding road: from mouse linkage studies to a novel human therapeutic pathway in type 1 diabetes, Front. Immunol. 13 (2022) 918837, https://doi.org/10.3389/fimmu.2022.918837.

[3] P.A. Lyons, W.W. Hancock, P. Denny, C.J. Lord, N.J. Hill, N. Armitage, T. Siegmund, J.A. Todd, M.S. Phillips, J.F. Hess, S.L. Chen, P.A. Fischer, L. B. Peterson, L.S. Wicker, The NOD Idd9 genetic interval influences the pathogenicity of insulitis and contains molecular variants of Cd30, Tnfr2, and Cd137, Immunity 13 (2000) 107–115, https://doi.org/10.1016/s1074-7613(00)00012-1.

[4] P.A. Lyons, N. Armitage, F. Argentina, P. Denny, N.J. Hill, C.J. Lord, M.B. Wilusz, L.B. Peterson, L.S. Wicker, J.A. Todd, Congenic mapping of the type 1 diabetes locus, Idd3, to a 780-kb region of mouse chromosome 3: identification of a candidate segment of ancestral DNA by haplotype mapping, Genome Res. 10 (2000) 446–453, https://doi.org/10.1101/gr.10.4.446.

[5] M.H. Forsberg, B. Foda, D.V. Serreze, Y.-G. Chen, Combined congenic mapping and nuclease-based gene targeting for studying allele-specific effects of Tnfrsf9 within the Idd9.3 autoimmune diabetes locus, Sci. Rep. 9 (2019) 4316, https://doi.org/10.1038/s41598-019-40898-8.

[6] J.L. Cannons, G. Chamberlain, J. Howson, L.J. Smink, J.A. Todd, L.B. Peterson, L. S. Wicker, T.H. Watts, Genetic and functional association of the immune signaling molecule 4-1BB (CD137/TNFRSF9) with type 1 diabetes, J. Autoimmun. 25 (2005) 13–20, https://doi.org/10.1016/j.jaut.2005.04.007.

[7] Y.-G. Chen, M.H. Forsberg, S. Khaja, A.E. Ciecko, M.J. Hessner, A.M. Geurts, Gene targeting in NOD mouse embryos using zinc-finger nucleases, Diabetes 63 (2014) 68–74, https://doi.org/10.2337/db13-0192.

[8] K. Kachapati, D.E. Adams, Y. Wu, C.A. Steward, D.B. Rainbow, L.S. Wicker, R. S. Mittler, W.M. Ridgway, The B10 Idd9.3 locus mediates accumulation of functionally superior CD137(+) regulatory T cells in the nonobese diabetic type 1 diabetes model, J. Immunol. 189 (2012) 5001–5015, https://doi.org/10.4049/jimmunol.1101013.

[9] M.H. Forsberg, A.E. Ciecko, K.J. Bednar, A. Itoh, K. Kachapati, W.M. Ridgway, Y.-G. Chen, CD137 plays both pathogenic and protective roles in type 1 diabetes development in NOD mice, J. Immunol. 198 (2017) 3857–3868, https://doi.org/10.4049/jimmunol.1601851.

[10] K. Kachapati, K.J. Bednar, D.E. Adams, Y. Wu, R.S. Mittler, M.B. Jordan, J. M. Hinerman, A.B. Herr, W.M. Ridgway, Recombinant soluble CD137 prevents type one diabetes in nonobese diabetic mice, J. Autoimmun. 47 (2013) 94–103, https://doi.org/10.1016/j.jaut.2013.09.002.

[11] B.M. Foda, A.E. Ciecko, D.V. Serreze, W.M. Ridgway, A.M. Geurts, Y.-G. Chen, The CD137 ligand is important for type 1 diabetes development but dispensable for the homeostasis of disease-suppressive CD137+ FOXP3+ regulatory CD4 T cells, J. Immunol. 204 (2020) 2887–2899, https://doi.org/10.4049/jimmunol.1900485.

[12] A. Itoh, L. Ortiz, K. Kachapati, Y. Wu, D. Adams, K. Bednar, S. Mukherjee, C. Chougnet, R.S. Mittler, Y.-G. Chen, L. Dolan, W.M. Ridgway, Soluble CD137 ameliorates acute type 1 diabetes by inducing T cell anergy, Front. Immunol. 10 (2019) 2566, https://doi.org/10.3389/fimmu.2019.02566.

[13] J. Michel, J. Langstein, F. Hofstädter, H. Schwarz, A soluble form of CD137 (ILA/4-1BB), a member of the TNF receptor family, is released by activated lymphocytes and is detectable in sera of patients with rheumatoid arthritis, Eur. J. Immunol. 28 (1998) 290–295, https://doi.org/10.1002/(SICI)1521-4141(199801)28:01<290::AID-IMMU290>3.0.CO;2-S.

[14] L. Yi, X. Jin, J. Wang, Z. Yan, X. Cheng, T. Wen, B. Yang, X. Wang, N. Che, Z. Liu, H. Zhang, CD137 agonists targeting CD137-Mediated negative regulation show enhanced antitumor efficacy in lung cancer, Front. Immunol. 13 (2022) 771809, https://doi.org/10.3389/fimmu.2022.771809.

[15] G. Zheng, B. Wang, A. Chen, The 4-1BB costimulation augments the proliferation of CD4+CD25+ regulatory T cells, J. Immunol. 173 (2004) 2428–2434, https://doi.org/10.4049/jimmunol.173.4.2428.

[16] A. Nowak, D. Lock, P. Bacher, T. Hohnstein, K. Vogt, J. Gottfreund, P. Giehr, J. K. Polansky, B. Sawitzki, A. Kaiser, J. Walter, A. Scheffold, CD137+CD154-expression as a regulatory T cell (Treg)-Specific activation signature for identification and sorting of stable human tregs from in vitro expansion cultures, Front. Immunol. 9 (2018) 199, https://doi.org/10.3389/fimmu.2018.00199.

[17] M.R. Alderson, C.A. Smith, T.W. Tough, T. Davis-Smith, R.J. Armitage, B. Falk, E. Roux, E. Baker, G.R. Sutherland, W.S. Din, Molecular and biological characterization of human 4-1BB and its ligand, Eur. J. Immunol. 24 (1994) 2219–2227, https://doi.org/10.1002/eji.1830240943.

[18] H. Schwarz, F.J. Blanco, J. von Kempis, J. Valbracht, M. Lotz, ILA, a member of the human nerve growth factor/tumor necrosis factor receptor family, regulates T-lymphocyte proliferation and survival, Blood 87 (1996) 2839–2845. http://www.ncbi.nlm.nih.gov/pubmed/8639902.

[19] J. Michel, S. Pauly, J. Langstein, P.H. Krammer, H. Schwarz, CD137-induced apoptosis is independent of CD95, Immunology 98 (1999) 42–46, https://doi.org/10.1046/j.1365-2567.1999.00851.x.

[20] W. Ren, G. Liu, J. Yin, B. Tan, G. Wu, F.W. Bazer, Y. Peng, Y. Yin, Amino-acid transporters in T-cell activation and differentiation, Cell Death Dis. 8 (2017) e2655, https://doi.org/10.1038/cddis.2016.222.

[21] M. Motamedi, L. Xu, S. Elahi, Correlation of transferrin receptor (CD71) with Ki67 expression on stimulated human and mouse T cells: the kinetics of expression of T cell activation markers, J. Immunol. Methods 437 (2016) 43–52, https://doi.org/10.1016/j.jim.2016.08.002.

[22] K. Luu, Z. Shao, H. Schwarz, The relevance of soluble CD137 in the regulation of immune responses and for immunotherapeutic intervention, J. Leukoc. Biol. 107 (2020) 731–738, https://doi.org/10.1002/JLB.2MR1119-224R.

[23] M. Setareh, H. Schwarz, M. Lotz, A mRNA variant encoding a soluble form of 4-1BB, a member of the murine NGF/TNF receptor family, Gene 164 (1995) 311–315, https://doi.org/10.1016/0378-1119(95)00349-b.

[24] S. Madireddi, S.-Y. Eun, S.-W. Lee, I. Nemčovičová, A.K. Mehta, D.M. Zajonc, N. Nishi, T. Niki, M. Hirashima, M. Croft, Galectin-9 controls the therapeutic activity of 4-1BB-targeting antibodies, J. Exp. Med. 211 (2014) 1433–1448, https://doi.org/10.1084/jem.20132687.

[25] A. Bitra, T. Doukov, J. Wang, G. Picarda, C.A. Benedict, M. Croft, D.M. Zajonc, Crystal structure of murine 4-1BB and its interaction with 4-1BBL support a role for galectin-9 in 4-1BB signaling, J. Biol. Chem. 293 (2018) 1317–1329, https://doi.org/10.1074/jbc.M117.814905.

[26] C. Becker, S. Wirtz, M.F. Neurath, Stepwise regulation of TH1 responses in autoimmunity: IL-12-related cytokines and their receptors, Inflamm. Bowel Dis. 11 (2005) 755–764, https://doi.org/10.1097/01.mib.0000172808.03877.4d.

[27] V. Dardalhon, T. Korn, V.K. Kuchroo, A.C. Anderson, Role of Th1 and Th17 cells in organ-specific autoimmunity, J. Autoimmun. 31 (2008) 252–256, https://doi.org/10.1016/j.jaut.2008.04.017.

[28] R. Luque-Martin, D.C. Angell, M. Kalxdorf, S. Bernard, W. Thompson, H.C. Eberl, C. Ashby, J. Freudenberg, C. Sharp, J. Van den Bossche, W.J. de Jonge, I. Rioja, R. K. Prinjha, A.E. Neele, M.P.J. de Winther, P.K. Mander, IFN-γ drives human Monocyte differentiation into highly proinflammatory macrophages that resemble a phenotype relevant to psoriasis, J. Immunol. 207 (2021) 555–568, https://doi.org/10.4049/jimmunol.2001310.

[29] Y.J. Kang, S.O. Kim, S. Shimada, M. Otsuka, A. Seit-Nebi, B.S. Kwon, T.H. Watts, J. Han, Cell surface 4-1BBL mediates sequential signaling pathways “downstream” of TLR and is required for sustained TNF production in macrophages, Nat. Immunol. 8 (2007) 601–609, https://doi.org/10.1038/ni1471.

[30] E. Littwitz-Salomon, I. Akhmetzyanova, C. Vallet, S. Francois, U. Dittmer, K. Gibbert, Activated regulatory T cells suppress effector NK cell responses by an IL-2-mediated mechanism during an acute retroviral infection, Retrovirology 12 (2015) 66, https://doi.org/10.1186/s12977-015-0191-3.

[31] F. Harris, Y.A. Berdugo, T. Tree, IL-2-based approaches to Treg enhancement, Clin. Exp. Immunol. 211 (2023) 149–163, https://doi.org/10.1093/cei/uxac105.

[32] A.K. Abbas, The surprising story of IL-2: from experimental models to clinical application, Am. J. Pathol. 190 (2020) 1776–1781, https://doi.org/10.1016/j.ajpath.2020.05.007.

[33] S.N. Sehgal, Sirolimus: its discovery, biological properties, and mechanism of action, Transplant. Proc. 35 (2003) 7S–14S, https://doi.org/10.1016/s0041-1345(03)00211-2.

[34] M.A. Hooks, Tacrolimus, a new immunosuppressant–a review of the literature, Ann. Pharmacother. 28 (1994) 501–511, https://doi.org/10.1177/106002809402800414.

[35] J.A. Singh, A. Hossain, A. Kotb, G. Wells, Risk of serious infections with immunosuppressive drugs and glucocorticoids for lupus nephritis: a systematic

review and network meta-analysis, BMC Med. 14 (2016) 137, https://doi.org/10.1186/s12916-016-0673-8.
[36] X. Chen, S. Li, D. Long, J. Shan, Y. Li, Rapamycin facilitates differentiation of regulatory T cells via enhancement of oxidative phosphorylation, Cell. Immunol. 365 (2021) 104378, https://doi.org/10.1016/j.cellimm.2021.104378.
[37] J. Kim, C.M. Hope, G.B. Perkins, S.O. Stead, J.C. Scaffidi, F.D. Kette, R.P. Carroll, S. C. Barry, P.T. Coates, Rapamycin and abundant TCR stimulation are required for the generation of stable human induced regulatory T cells, Clin. Transl. Immunol. 9 (2020) e1223, https://doi.org/10.1002/cti2.1223.
[38] M. Battaglia, A. Stabilini, M.-G. Roncarolo, Rapamycin selectively expands CD4+ CD25+FoxP3+ regulatory T cells, Blood 105 (2005) 4743–4748, https://doi.org/10.1182/blood-2004-10-3932.
[39] L. Strauss, T.L. Whiteside, A. Knights, C. Bergmann, A. Knuth, A. Zippelius, Selective survival of naturally occurring human CD4+CD25+Foxp3+ regulatory T cells cultured with rapamycin, J. Immunol. 178 (2007) 320–329, https://doi.org/10.4049/jimmunol.178.1.320.
[40] C. Scottà, M. Esposito, H. Fazekasova, G. Fanelli, F.C. Edozie, N. Ali, F. Xiao, M. Peakman, B. Afzali, P. Sagoo, R.I. Lechler, G. Lombardi, Differential effects of rapamycin and retinoic acid on expansion, stability and suppressive qualities of human CD4(+)CD25(+)FOXP3(+) T regulatory cell subpopulations, Haematologica 98 (2013) 1291–1299, https://doi.org/10.3324/haematol.2012.074088.
[41] L. Passerini, F. Barzaghi, R. Curto, C. Sartirana, G. Barera, F. Tucci, L. Albarello, A. Mariani, P.A. Testoni, E. Bazzigaluppi, E. Bosi, V. Lampasona, O. Neth, D. Zama, M. Hoenig, A. Schulz, M.G. Seidel, I. Rabbone, S. Olek, M.G. Roncarolo, M. P. Cicalese, A. Aiuti, R. Bacchetta, Treatment with rapamycin can restore regulatory T-cell function in IPEX patients, J. Allergy Clin. Immunol. 145 (2020) 1262–1271.e13, https://doi.org/10.1016/j.jaci.2019.11.043.
[42] C.M. Hull, M. Peakman, T.I.M. Tree, Regulatory T cell dysfunction in type 1 diabetes: what's broken and how can we fix it? Diabetologia 60 (2017) 1839–1850, https://doi.org/10.1007/s00125-017-4377-1.
[43] Y. Zhao, S. Wei, L. Chen, X. Zhou, X. Ma, Primary biliary cholangitis: molecular pathogenesis perspectives and therapeutic potential of natural products, Front. Immunol. 14 (2023) 1164202, https://doi.org/10.3389/fimmu.2023.1164202.
[44] W. Li, C. Deng, H. Yang, G. Wang, The regulatory T cell in active systemic lupus erythematosus patients: a systemic review and meta-analysis, Front. Immunol. 10 (2019) 159, https://doi.org/10.3389/fimmu.2019.00159.